Review / Pregledni znanstveni članak

Peculiarities of the Use of Visualization Systems on UAV Platforms for Remote Gamma Monitoring

Sergiy KRYACHOK – Chernihiv[1], Vadym BELENOK, Dmytro LIASHENKO – Kyiv[2], Liliia HEBRYN-BAIDY – Cambridge[3], Roman TRETIAK, Olena BOYKO – Kyiv[2]

ABSTRACT. Currently, the threat of nuclear weapons use has increased, with their deployment in new regions, and there are risks of accidents at nuclear power plants and terrorist acts involving nuclear charges. Therefore, remote gamma monitoring is relevant. The ability of UAVs to fly at low altitudes and speeds allows to increase the reliability of gamma monitoring compared to space and manned remote sensing means and to protect UAV operators from radiation exposure compared to ground-based methods, while visualization of monitoring results provides two- or three-dimensional models of radiation distribution on the earth's surface. A review of radiation imaging systems is made: with collimated detectors, with coded aperture, with rotational modulation, Compton imaging, with moving detectors (directional systems). Due to the smallest size and weight characteristics and the ability to operate in a remote gamma field, only the last two systems are currently suitable for use on UAVs. It has been established that systems with movable detectors on UAV platforms allow gamma monitoring in full: search for radioactive sources, mapping of natural radiation background and areas contaminated with radionuclides. Currently, Compton imaging sys-

[1] Assoc. Prof. Sergiy Kryachok, PhD, Department of Geodesy, Cartography and Land Management, Chernihiv Polytechnic National University, Shevchenko Street 95, UA-14035 Chernihiv, Ukraine, e-mail: geodesist2015@gmail.com

[2] Assoc. Prof. Vadym Belenok, PhD, corresponding author, Aerospace Geodesy and Land Management Department, State University "Kyiv Aviation Institute", Liubomyra Huzara Ave. 1, UA-03058 Kyiv, Ukraine, e-mail: vadym.belenok@npp.kai.edu.ua
Prof. Dr. Dmytro Liashenko, Geoinformatics Department, Taras Shevchenko National University of Kyiv, Institute of Geology, Vasylkivska str. 90, UA-03022 Kyiv, Ukraine, e-mail: uageog@gmail.com
Assoc. Prof. Roman Tretiak, PhD, Aerospace Geodesy and Land Management Department, State University "Kyiv Aviation Institute", Liubomyra Huzara Ave. 1, UA-03058 Kyiv, Ukraine, e-mail: roman.tretiak@npp.kai.edu.ua
Senior Lecturer Olena Boyko, Aerospace Geodesy and Land Management Department, State University "Kyiv Aviation Institute", Liubomyra Huzara Ave. 1, UA-03058 Kyiv, Ukraine, e-mail: olena.boiko@npp.kai.edu.ua

[3] Fellow Researcher Liliia Hebryn-Baidy, PhD, Scott Polar Research Institute, Department of Geography, University of Cambridge, Cambridge CB2 1ER, UK, e-mail: lh825@cam.ac.uk

tems allow detection of radiation sources at lower altitudes and speeds, which makes them effective for searching for sources in local areas of the urban environment and indoors, but does not allow mapping of large areas of radiation contamination.

Keywords: imaging systems, gamma radiation, remote sensing, UAVs, gamma detectors, radiation monitoring.

1. Introduction

The main task of unmanned vehicles (UVs) is to replace humans (pilots) during missions that are dangerous to their health and life.

The use of surface UVs is known. The main areas of their use are reconnaissance missions, protection of water areas from combat swimmers and scouts, remote mining and attacks on enemy ships and infrastructure facilities (Galushko 2023).

Underwater UVs are used to create passages through sea minefields (URL 1).

Ground-based UVs are used for cleaning apartments and yards, and in agriculture – for precision farming, field inspection, and delivery of materials to the farm (URL 2). Unmanned robotic systems are also used to perform levelling of airfield runways (Burachek et al. 2018, Tereshchuk et al. 2021). In the military, ground-based UVs are used for reconnaissance, combat use, and transporting the wounded from the battlefield (Zhyrokhov 2017).

Among the UVs, unmanned aerial vehicles (UAVs) are currently the most functional. They have been used in forestry to determine the characteristics of a stand of trees and to search for fire sites (Adão et al. 2017). In agriculture, UAVs are used for: monitoring the condition of agricultural land; operational assessment of land conditions; and yield forecasting (Zhang et al. 2019). Large-scale aerial surveys of small areas and the creation of digital terrain models of underwater areas of water bodies based on the results of aerial surveys are performed by UAVs (Silwal et al. 2022). On the battlefield, UAVs reconnoiter enemy positions and adjust artillery fire, while kamikaze UAVs perform fire on critical infrastructure, air defence assets, armoured targets, and concentrations of personnel (Korsunov et al. 2021). UAVs are constantly improving their element base and navigation tools (Tereshchuk et al. 2023).

Over the past decades, humanity has faced large-scale consequences of accidents at nuclear power plants in Ukraine – in Chornobyl and Fukushima – in Japan. Currently, the threat of nuclear weapons use, their deployment in new regions, and the risk of accidents at nuclear power plants as a result of terrorist acts has increased, which could lead to radiation contamination of the territories.

Therefore, it is relevant to develop remote sensing tools for monitoring radioactive radiation on UAV platforms aimed at finding sources of radioactive radiation, mapping natural elevated radiation background or areas contaminated with radionuclides (Widodo et al. 2020). The small dimensions and weight characteristics of UAVs made it possible to significantly reduce the cost of their use, and the ability to fly at low altitudes and low speeds made it possible to increase the reliability of the results obtained regarding the distribution fields of ground radiation compared to space and manned aircraft and to protect UAV operators from direct exposure to the territory of radiation contamination and to speed up the acquisition of monitoring results compared to ground-based methods (Van der Veeke et al. 2021).

Gamma radiation is at the end of the short-wave, high-energy range of electromagnetic radiation with a wavelength of less than $2 \cdot 10^{-10}$ m. This radiation is the most penetrating among the types of radioactive radiation (Gordon 2008). Therefore, airborne radiation monitoring systems are aimed at detecting gamma radiation.

The aim of the article is to review the peculiarities of using imaging systems on the following platforms UAVs for remote gamma monitoring.

2. Radiation Imaging Systems

UAV technologies for gamma monitoring include detection of the territory and computer processing of counting and spectral information on radiation to obtain its optical representation, and therefore belong to visualization methods ((Makhnov 2019a). In addition to the above, gamma-ray imaging of the radiation contamination area involves coordinate-oriented documentation of the optical representation of the distribution of gamma radiation on the earth's surface using cartographic materials.

Various radiation detectors are used in imaging systems. Their operation is based on the fact that the ingress of a high-energy nuclear particle into a material environment leads to its ionisation. Detectors are differentiated by the method of detecting ionized fluxes. For example, in a Geiger-Muller detector, at a high voltage of 500 V to 800 V between the anode and cathode and the presence of an inert gas inside the cylinder, a gas amplification phenomenon is induced, which accelerates free electrons from initial ionization to the appearance of an uncontrolled chain avalanche throughout the gas volume, generating an electrical pulse or countdown. This process lasts from 200 μs to 400 μs, during which time the detector is considered 'dead' and unable to detect new nuclear particles before it can start counting pulses again. To reduce the dead time, for example, 10% ethanol is added to the gas tube. The detector records the radiation intensity by the count rate (Ahmad et al. 2021, Molnar et al. 2021).

A scintillation detector uses the property of the material medium to absorb energy from a charged particle, which leads to the emission of light – scintillation. For this purpose, crystalline scintillators such as sodium iodide (NaI), zinc sulphide (ZnS) and others are used. The ultraviolet light generated in the scintillator is focused on the photocathode, causing a photographic effect that is amplified, for example, by a photomultiplier tube. The signal from the scintillation detector is proportional to the energy of the detected gamma photon, and the count rate, which corresponds to the frequency of light flashes, records the radiation intensity (Ahmad et al. 2021, Molnar et al. 2021).

In a semiconductor detector, incident radiation causes electron-hole pairs to appear in the semiconductor, resulting in a detection signal. These detectors can operate at low voltages, have low power consumption, are less sensitive to electromagnetic fields, and are much smaller in size and, due to the high density of the solid state, can provide more information about the incident radiation than other types of detectors (Ahmad et al. 2021, Molnar et al. 2021).

Important properties of radiation imaging systems are field of view, spatial resolution, energy resolution, and noise. The field of view is the solid angle within which the detector collects radiation. Spatial resolution determines the detail of the image object. Energy resolution determines how well individual gamma lines in the energy spectrum can be distinguished from other lines and the background. Noise, i.e. statistical noise due to random fluctuations in radioactive decay or systematic noise, for example, due to instrumental artefacts (Ahmad et al. 2021).

Existing methods of gamma field imaging are divided into the following groups: systems with collimated detectors; systems with coded aperture; systems with rotational modulation; Compton imaging systems; systems with moving detectors, or directional systems (Makhnov 2019a, Vetter et al. 2006).

In imaging systems with collimated detectors, position-sensitive detectors are used as a sensing element – matrices or arrays of individual radiation detectors or continuous scintillator crystals with a flash position registration system (Makhnov 2019a). For example, an Anger chamber contains a heavy absorber made of lead or tungsten alloys with many holes placed in front of a position-sensitive gamma-ray detector (Fig. 1). The spatial resolution of the system depends on the distance of the detectors to the absorber and the diameter of the hole in it. However, at distances of several tens of meters, the resolution deteriorates to the point where no structure can be distinguished within the field of view, since the gamma radiation source is visible through all the collimator apertures. In this case, such a system is transformed into a tube collimator, and provides the ability to obtain images only by moving the system (Vetter et al. 2006).

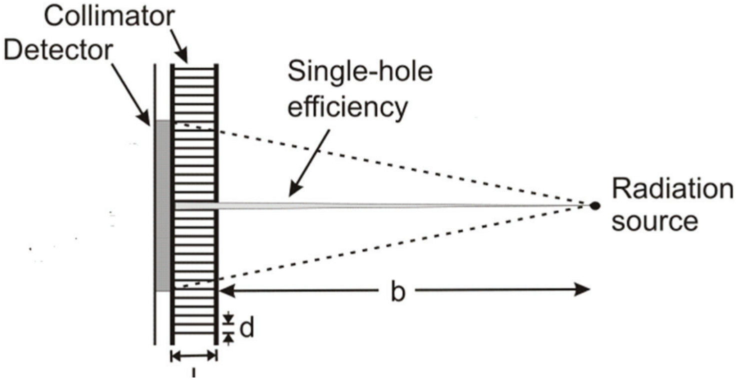

Fig. 1. *Anger chamber: a collimator with a detector and a system of parallel apertures of length l and diameter d, located at a distance b from the radiation source (Vetter et al. 2006).*

To improve efficiency and increase the field of view, collimators have been developed in the form of a flat mask with many holes that form a coded aperture. Coded aperture systems uniquely modulate each position in the field of view to a position-sensitive gamma radiation detector. The resulting image must be decoded using digital or optical methods. Fig. 2 shows a diagram of a coded aperture system in the form of a gamma scanner. The efficiency of its use is limited in conditions of high activity and complex gamma background. A coded aperture system can only reduce the intensity of the background above the signal, but cannot completely distinguish between them, especially for imaging long objects. For long distances of several tens of meters, coded aperture is equivalent to a simple point system. Coded aperture systems are very heavy (Amgarou et al. 2016, Makhnov 2019b, Vetter et al. 2006).

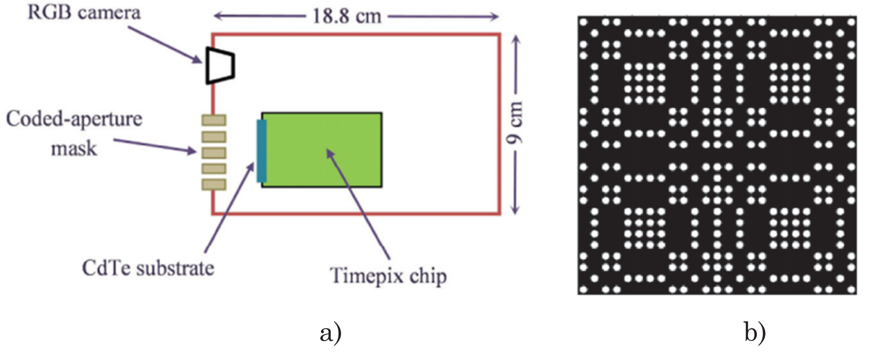

Fig. 2. *Gamma scanner: a) optical camera, coded aperture mask, CdTe detector (cadmium telluride), Timepix chip for detecting radioactive photons (Amgarou et al. 2016); b) view of the coded aperture mask made of tungsten (Paradiso et al. 2017).*

Systems with code modulation can use the principle of 'mask-antimask' (Fig. 3a). To implement such a system, it is necessary to have a mask composed of several periods of a uniformly redundant array, the location of each of the detectors opposite a single element of the mask, and the ability to turn the mask into an anti-mask by rotating it by 180°. This allows compensating for uneven background exposure of the detectors. The system can work with gamma radiation sources located at considerable distances – with parallel beams (Vetter et al. 2006).

A rotationally modulated system can consist of two sets of parallel gratings made of shielding material (rotationally modulated collimator) (Fig. 3b). Both gratings are rotated together in front of the detector, modulating the incoming radiation. Thus, the intensity of the radiation depends on the angle of the signal entering the system and on the current angle of rotation of the gratings and can be reproduced using an appropriate algorithm. The system does not require a position-sensitive gamma detector. Depending on the design and energies, the resolution can vary from 1° to several arc seconds. Rotationally modulated systems are very heavy (Makhnov 2019b, Vetter et al. 2006).

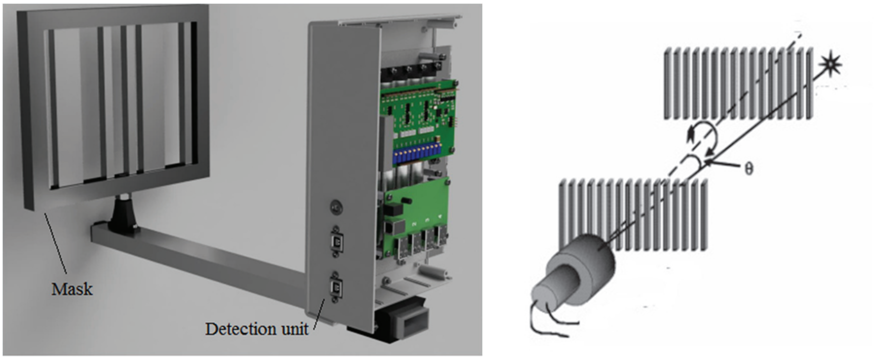

a) b)

Fig. 3. *Systems requiring rotation of masks: a) 'mask-antimask' system (Makhnov 2019b); b) system with rotational modulation (Vetter et al. 2006).*

The concept of Compton imaging is based on the process of Compton scattering and the relationship between the scattering angle θ and the energy of the incident gamma radiation (Fig. 4a) (Vetter et al. 2006). The Compton imaging system, unlike conventional and collimator imaging systems, requires that the incident gamma radiation interacts at least twice in the detector: once by Compton scattering and once by photoelectric absorption. The positions of the first two interactions define the symmetry axis of the cone, whose opening angle θ is determined by the energy of the first interaction and the total energy of the gamma radiation. The projections of the cones onto the sphere will overlap at the location of the source (Fig. 4b), which allows determining its position in three dimensions.

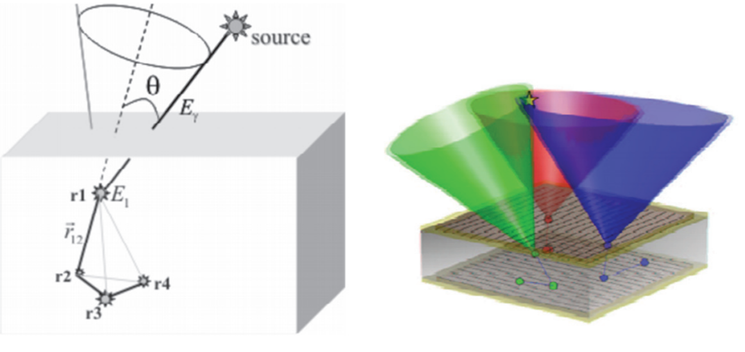

a) b)

Fig. 4. *Illustration of the Compton imaging principle: a) relationship between the scattering angle and the energy of incident gamma radiation; b) intersection of scattering cones (Vetter et al. 2006).*

Compton imaging systems are the only ones that can distinguish between background and source because they can measure both simultaneously. Advances in two-dimensional segmentation of semiconductor detectors and signal processing have made it possible to create effective high-resolution Compton imaging systems. The disadvantage of Compton imaging is their complexity and potentially high cost (Vetter et al. 2006).

Systems with moving detectors are simple devices consisting of position-insensitive detectors. They allow the location of sources to be determined provided that the detection system or the source is moving. Systems can have directional or omnidirectional detectors. The angle of the field of view ω corresponds to the value of the spatial resolution. Detectors can be shielded. The shielding creates a shadow that allows for more accurate and reliable source location than is possible with an unshielded detector. Such a directional detector usually has the form of a collimator tube (Fig. 5a). The angle of the field of view ω and the height *H* determines the field of view – the diameter *D* of the area on the earth's surface from which radiation is received by the detector (Fig. 2b). These systems are capable of operating in the far radiation field (Makhnov 2019a).

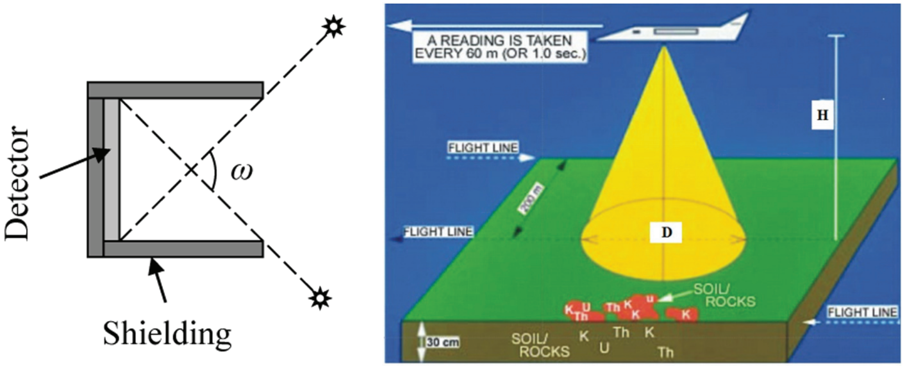

a) b)

Fig. 5. *To the system with a mobile detector: a) field of view angle of the directional detector (Kryachok 2024); b) imaging system with a mobile airborne detector (Makhnov 2019a).*

A summary of the main technical parameters of the imaging systems is given in Table 1. The energy resolution depends on the type of detector (Vetter et al. 2006).

Table 1. *Summary of performance and engineering parameters of the five gamma-ray imaging categories (Vetter et al. 2006).*

Parameters	Collimator	Coded Aperture	Rotation Modulation	Compton Camera	Directional
FOV	< 60°	< 60°	< 60°	180° or 360°	30° – 360°
Angular Resolution	< 30°	< 5°	< 5°	1° – 5°	> 30°
Energy Resolution	Very Poor – Excellent	Very Poor – Excellent	Very Poor – Excellent	Good – Excellent	Very Poor – Excellent
Minimum Weight	20 kg	20 kg	20 kg	0.5 kg	0.1 kg

As noted above, systems with collimated detectors and coded apertures lose their distinguishing properties in the far radiation field. Systems with coded and rotational modulation have significant dimensions and weight. According to Table 1, Compton imaging systems and systems with movable detectors have the lowest weight compared to other imaging systems and are able to operate in the remote radiation field. Therefore, it is clear that systems with moving detectors and Compton imaging are the most suitable for use on UAVs.

3. Imaging Systems with Moving Detectors on UAV Platforms

Article (Burtniak et al. 2018) presents data on the remote radiation monitoring system. It consists of three subsystems: UAV in the form of an octocopter; radiation monitoring subsystem (GR-Smart) installed on the octocopter and ground subsystem (Fig. 6).

The main structural elements of the UAV are: a control system consisting of a manual control subsystem and an automatic control subsystem (autopilot); a gyro-stabilised platform on which the GR-Smart is placed; orientation, speed and direction sensors and a GPS receiver; and a radio communication channel with the ground subsystem.

The onboard remote sensing subsystem GR-Smart stores the following data during the flight: geographical coordinates, altitude, pressure, temperature and spectrometric data.

The ground-based subsystem is computerised and performs the following functions: data processing; database maintenance; construction of radionuclide spectra and counts per second; detection of local radioactive contamination zones; determination of gamma radiation dose rate; determination of coordinates of point sources of gamma radiation; construction of a contour map of gamma radiation distribution and documentation of radiation monitoring data; data reception via Wi-Fi from GR-Smart.

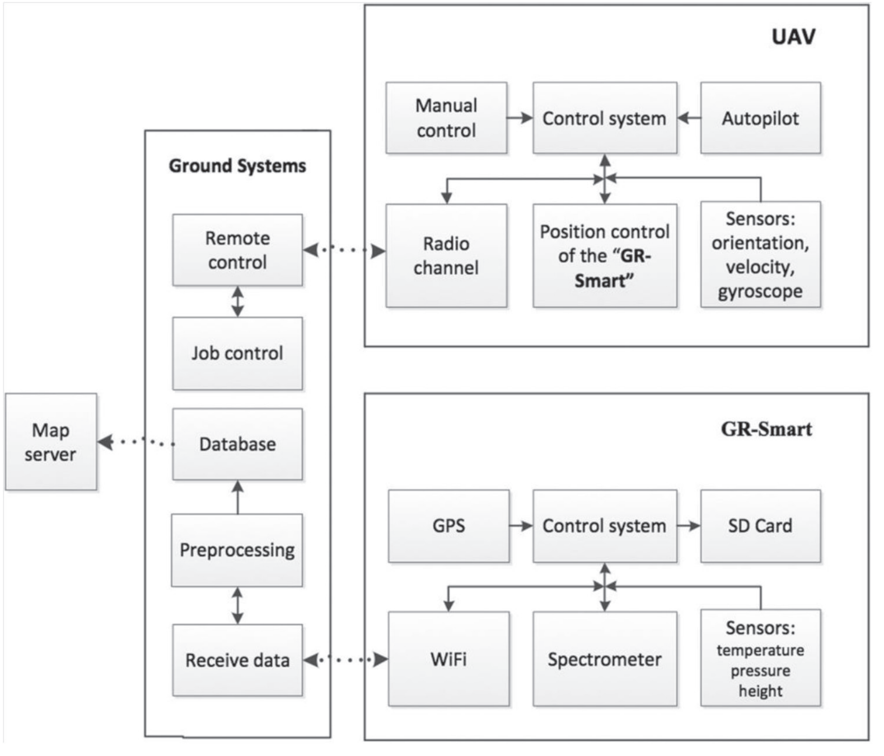

Fig. 6. *Remote radiation monitoring systems flowchart (Burtniak et al. 2018).*

The main element of GR-Smart is a NaI (T1) gamma-ray spectrometer. The spectral information is accumulated in the form of amplitude-time. The detection system consists of five detectors, the characteristics of which are shown in Table 2.

Table 2. *Characteristics of the radiation detector and gamma-ray imaging conditions (Burtniak et al. 2018).*

Detector	**5 scintillators NaI (T1) 63 to 63 mm**
Dose rate sensitivity	0.8 μSv·h^{-1}
Sensitivity of surface contamination density	0.5 kBq·m^{-2}
Energy range	from 30 to 3000 keV
Relative energy resolution for Cs137	0.1 sec
Data collection frequency	10 Hz
UAV speed	2.8 m·c^{-1}
Flight height	from 5 to 30 m

Information from five detectors is synchronized in one integrated detector. The Wi-Fi data channel transmits data in real time over a distance of up to 1 km. The on-board GR-Smart subsystem is capable of surveying 3 km^2 per hour. The flight time is 40 minutes. Battery replacement takes 5 minutes. Therefore, the UAV can survey up to 21 km^2 in one day.

Paper (Zabulonov et al. 2017) presents data on an automated rapid response system for radiation control and environmental monitoring. The system consisted of a UAV and a ground station. The detector is based on a 63 × 63 mm Nai (Tl) crystal weighing 0.85 kg with an energy resolution of 6% and a photomultiplier tube. The detection unit weighs 6.5 kg and contains 5 detectors. In areas with high radiation activity, one or more basic detectors are switched off. Conversely, if the radiation activity of the site is low, the statistical reliability of the measurement is increased by connecting additional basic detectors.

From the UAV, the following is performed: measurement and collection of gamma radiation spectra from the earth's surface, identified by geographical coordinates and altitude; visualization of the area using a survey camera. The information is transmitted to the station at one-second intervals via a WiFi communication channel.

The screen of the ground station based on the vehicle displays the following data in real time: aircraft coordinates automatically obtained from the GPS satellite navigation system unit; spectral composition of radioactive contamination attributed to real objects; dose and power of the equivalent dose of radioactive radiation. The measurement range is: photon radiation energy 0.5–3000 keV; equivalent dose rate 0.1–5000 µSv/h. ArcGIS software was used to process the gamma-ray data, and the empirical Bayesian kriging method was used for interpolation. The following tasks are also performed: documentation of the obtained radiation monitoring data; construction of a map-scheme at a scale of 1:10 000 (Fig. 7) (Zabulonov et al. 2017).

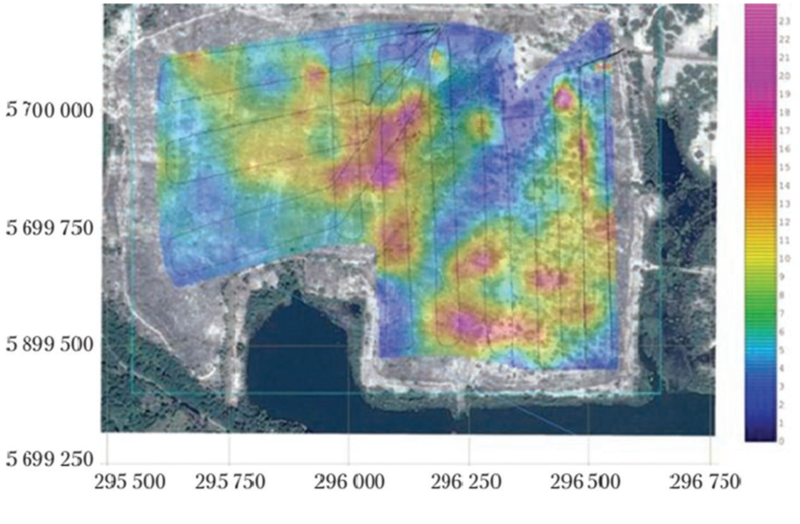

Fig. 7. *Map of equivalent dose intensity on the scale 1:10 000 (Zabulonov et al. 2017).*

A gamma-ray spectrometry system on a UAV platform for the reconnaissance and identification of natural radionuclides is presented in (Kunze et al. 2022). The system included $CeBr_3$ (Medusa) scintillation detector (7.5 × 15 mm) with a resolution of 3.9% for 662 keV; global navigation satellite system (GNSS); compass; inertial measurement unit and gyro sensors; laser range finder; temperature and pressure sensors; first person view camera; communication systems.

The identification of natural radionuclides was carried out at an outdated uranium mining site in Mailuu Suu in southern Kyrgyzstan. The UAV flew at an altitude of 10 m above sea level at a speed of 3 m/s. The distance between the survey lines was 10 m. The UAV was hovering in the hot spots. During the flight, raw spectra, GPS data, and time stamps were recorded on a USB device that could be removed from the spectrometer. Data processing was performed on a personal computer. Data processing is carried out at two levels: the total spectrometer reading rate and spectrometric data. For spectral analysis, the window method and, alternatively, the full spectrum analysis method were used. The software used to create the maps was the spline interpolation method. Color maps of increased radionuclide activity or decay series were created for: K-40, U-238, Th-232. Google Earth contour maps served as the basis for creating radioactivity maps of the study area.

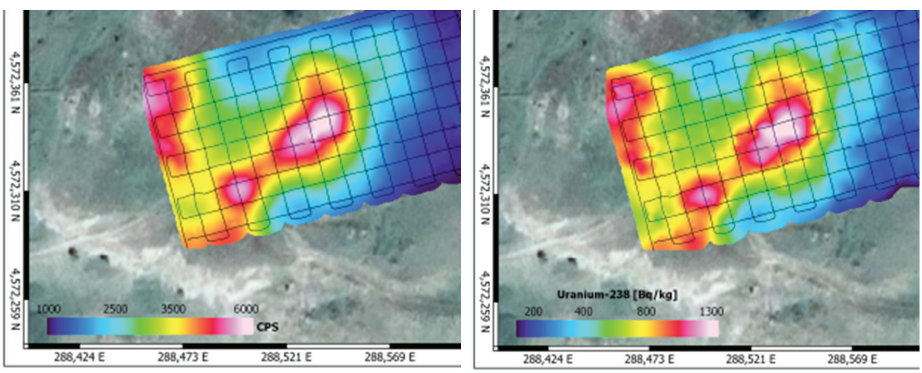

a) b)

Fig. 8. *Gamma survey results: a) total count rate in the study area; b) specific activity of U-238 in the study area (Kunze et al. 2022).*

Fig. 8, a shows the total count rate in counts per second (cps) without any processing, except spline interpolation of the data points. Fig. 8 shows the results of data processing, i.e., the specific activities in Becquerels per kilogram of U-238 decay series, respectively. These results have been calculated with the full spectrum method (Kunze et al. 2022).

Paper (Woodbridge et al. 2023) provides information on the use of vertical takeoff and landing UAVs with fixed wings for airborne gamma-ray mapping (Fig. 9a). VTOL allows collecting radiometric data over many kilometers of territory much faster than multi-rotor UAVs. Such a system is useful for responding to nuclear accidents when terrain mapping, mineral exploration and mine site surveys are urgently needed. The VTOL is a commercial Wingtra one, weighs 4.5 kg, has a cruising speed of 60 km per hour, carries a payload of 800 g, has a flight time of 55 minutes, and is resistant to winds of 45 km per hour. The payload includes a GPS receiver and an autonomous airborne radiation mapping system (AARM), which is installed in place of a standard DSLR camera. The AARM system consists of a CsI(Tl) scintillator; a semiconductor detector based on cadmium-zinc telluride (a Cadmium Zinc Telluride) to add gamma-ray mapping capabilities for energies above 1.4 MeV; and a GPS receiver. The UAV has a standard downward-facing LIDAR and power supply. Radiological data is stored and transmitted via cellular communication to obtain real-time data (Woodbridge et al. 2023).

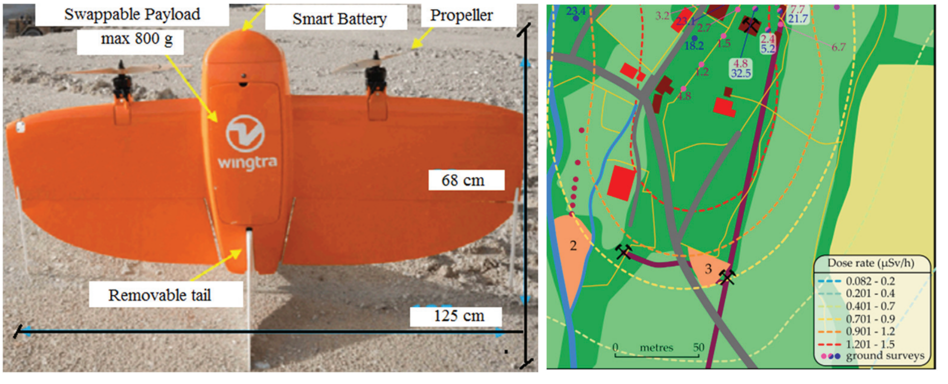

a) b)

Fig. 9. *UAVs with vertical take-off and landing with a fixed wing and results of gamma-ray survey: a) UAV body containing a payload of up to 800 g, a replaceable tail, a 'smart' battery, a propeller; b) map of the area with the distribution of gamma radiation dose rate (Woodbridge et al. 2023).*

An old uranium mine was used to test the VTOL system. The flights were performed in tack in automatic mode at an altitude of 70 m at a speed of 15 m/s with an interval between tacks of 20 m. The gamma spectra were collected at a frequency of 10 Hz, which were combined into larger time intervals of 1, 2, and 5 Hz during post-processing. The peak intensities were calculated using the spectral window method for the corresponding photon energies with the contribution of scattered photons removed. Spectral intensities were converted to equivalent dose rates. Each measurement was corrected for the difference in height above ground level using the height recorded by the onboard LiDAR and taking into account the linear attenuation coefficient of air with standard temperature and pressure for the corresponding photon energies and brought to a height of 1 m above the ground surface. The processed data was visualized in ArcGIS Pro with interpolation of radiometric data using the Empirical Bayesian Kriging tool. As a result, a map of the area with the distribution of dose rates on the territory of the uranium mine in the form of isolines of equal dose rate was obtained (Fig. 9b) (Woodbridge et al. 2023).

The system for detecting radiation contamination of the area is described in (Molnar et al. 2021). The system consisted of a UAV, a GPS receiver, and subsystems for radiation detectors, data recording, data processing, and visualization. Moreover, two different detector subsystems were tested based on Geiger-Muller counters and a scintillation detector. The scintillation detector subsystem contained a 13 × 13 × 47 mm CsI (Tl) crystal and a multipixel photon counter.

To search for the source of radiation contamination, the territory was conditionally divided into squares with a side of 3 × 3 m. On the planned route, the UAV hovered for 10 seconds in the center of each square, the coordinates of the point were determined, and gamma radiation measurements were performed every second. The data recorded during the flights were processed offline using the developed MATLAB software, after which the results were visualized. The gamma radiation source was made up of autunite minerals $(Ca(UO_2)_2(PO_4)_2 \times (10\sim12)H_2O)$ distributed on a 30 cm diameter disc. The measurements were performed from a height of 3 meters, as this was the optimal height for detecting a low-power source. In the unfiltered data set, it is difficult to find signs of a source among the background radiation, and several false peaks appear. However, visualization of the gamma radiation intensity from the measurement data in the form of a flat distribution allows us to clearly separate the source from the background radiation (Fig. 10) (Molnar et al. 2021).

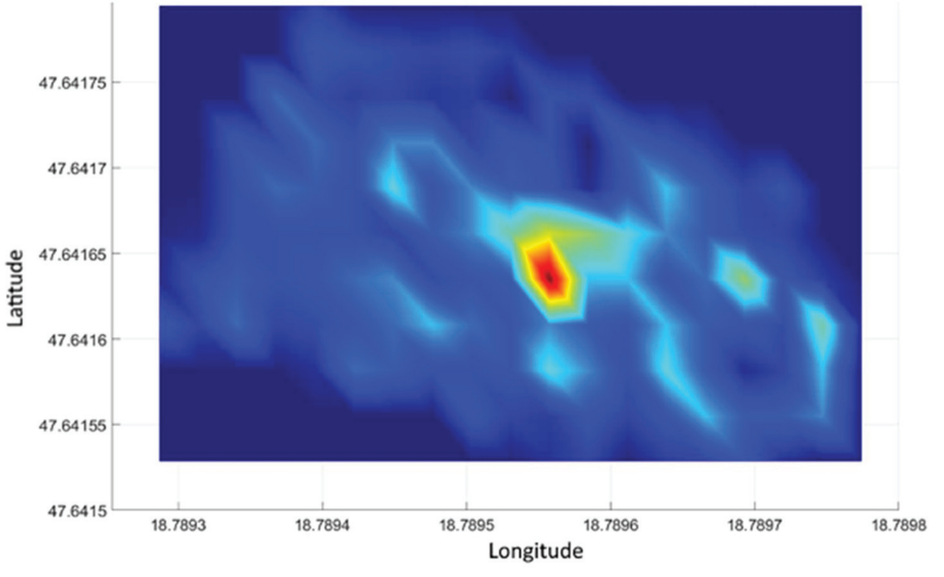

Fig. 10. *Distribution of gamma radiation intensity in the experimental area (Molnar et al. 2021).*

The system for detecting gamma radiation sources with an advanced radiation detector for UAV operations (ARDUO), for placement on a UAV platform in the form of a helicopter with a payload of up to 6 kg, is presented in (Chen et al. 2020). The system includes a barometer, GNSS receiver, compass, and inertial measuring device to determine its position and orientation every 0.02 seconds. The ARDUO detector has 8 CsI(Tl) crystals measuring 2.8 cm × 2.8 cm × 5.6 cm, placed in a self-shielded configuration, with silicon photomultipliers. Each gamma radiation detector in the 2 × 2 detector array has partial attenuation of the radiation signal through neighboring detectors, which allows determining the azimuth and elevation angle in the direction of the radiation source. The UAV's autopilot records latitude, longitude, altitude and orientation using an advanced Kalman filter and a set of listed sensors, providing each radiation measurement with a position and coordinates for further analysis. The information is transmitted to the operator's control station every second (Fig. 11). The nominal flight parameters of the ARDUO for the search for the radiation source were: altitude 10 m, speed 2 m/s, tack distance 4 m. The directional reconstruction algorithm allows for real-time results for any spectrum prior to isotope identification and is effective in locating even highly shielded isotopes or mixed radiation fields due to its wide energy range from 0.1 MeV to 3.0 MeV.

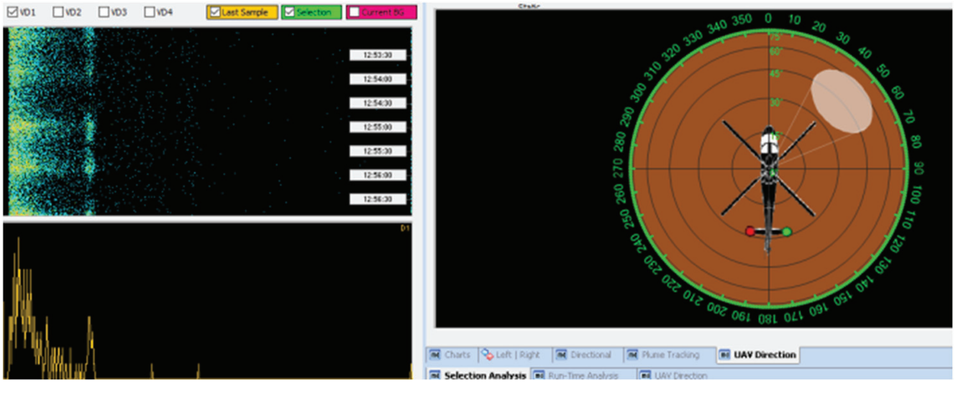

Fig. 11. *Viewing data on real-time operator displays over the* ^{137}Cs *gamma source: the upper left display on the vertical axis shows time; energy on the horizontal axis; its amount in the display plane; the lower left display shows the current one-second energy spectrum for one detector (for isotope identification); the right display shows the current reconstruction of the direction pointing to the source at an azimuth of 50° and an elevation angle of about 45° (Chen et al. 2020).*

The Localization and Mapping Platform (LAMP) for the search for gamma radiation sources to eliminate the consequences of radioactive material releases is presented in (Pavlovsky et al. 2018). The LAMP platform is self-sufficient, i.e. it can be deployed in portable configurations or on unmanned ground or air vehicles, as well as in manual configurations. The modularity of the LAMP system allows sensor combinations to be configured to meet specific use cases. The platform includes: LiDAR, four commercial CsI (Tl) scintillation detectors weighing about 0.6 kg, a survey camera, an autonomous navigation system

IMU, a GPS receiver, an on-board computer, a communication channel, a battery (Fig. 12a), and a multi-copter UAV. Each gamma radiation detector in the 2 x 2 detector array has a partial attenuation of the radiation signal due to neighboring detectors. This causes a self-shielding effect. It helps to determine the direction of the radiation source. As a result, LAMP allows gamma mapping using the 'scene data fusion' function, which combines radiation data and terrain data using a voxelized 3-dimensional method of maximization the mathematical expectation of likelihood to create 3-dimensional maps of the distribution of radioactive sources in real time (Fig. 12b).

The results are calculated on board the LAMP during the UAV's flight and transmitted via a communication channel to the user, who can view a three-dimensional map on a tablet in real time. Since the angular resolution of the system is low, the proximity effect was used for localization. In the reported cases, the LAMP proximity distance was 1–3 m, which allows for a spatial resolution of several meters (Pavlovsky et al. 2018).

The technology for creating contour maps of radiation contamination areas and detecting radiation sources using a swarm of UAVs is presented in (Kazemeini et al. 2019). This technology allows to automatically determine the contamination contour using a swarm of UAVs without entering the exposure zone directly. Gamma data from each UAV is time-stamped and combined with location data and transmitted via a communication channel to a ground station. Radiation sensors were installed on each UAV platform: a semiconductor cadmium-zinc telluride sensor or an elpasolite scintillation sensor.

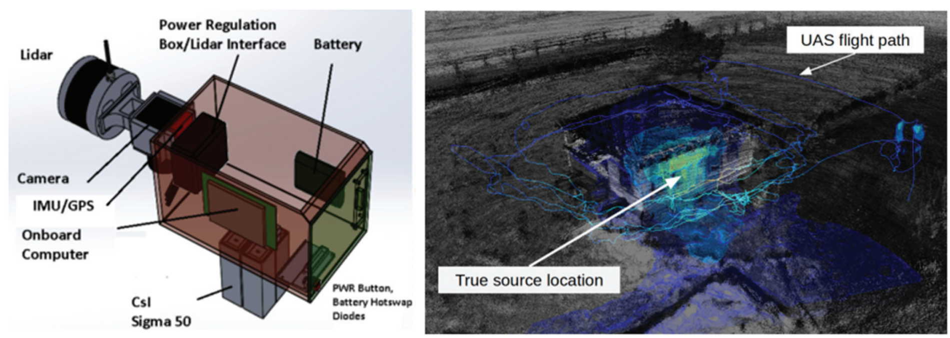

a) b)

Fig. 12. *The Localisation and Mapping Platform (LAMP) and gamma-ray survey results: a) platform payload; b) 3-dimensional map of radiation distribution with the source inside the building (Pavlovsky et al. 2018).*

The CZT sensor for gamma-ray spectrometry has a high energy resolution (less than 2% for photon energy of 662 keV). It operates in direct conversion mode at ambient temperature and contains a 1 cm^3 CZT crystal. The energy range of the sensor is from 30 keV to 3 MeV. The data array from the CZT sensor is sent via USB to an on-board mini-computer, where a gamma radiation spectrum is generated and then analyzed using a code to identify peaks in the presence of background in the measured spectrum. The peaks are approximated using a

Gaussian function. This allows the identification of the isotopes emitting these gamma rays and the estimation of the source power (Kazemeini et al. 2019).

The CLYC detector is used for neutron and gamma measurement identification. The CLYC sensor is constructed of a cylindrical crystal with a diameter of 2.54 cm and a length of 2.54 cm. The wavelength range of its scintillation radiation is from 275 to 450 nm. This crystal is combined with a superbicallium photomultiplier tube, a miniature digitizer and a high voltage generator. All this was packed into a special case (Fig. 13a). The sensor operates without cooling. The measured energy resolution of gamma quanta was 5% at 662 keV and 3.3% at 1332 keV. Neutron signals appear at energies of 3200 keV. The graph in Fig. 13b shows that neutron and gamma signals are well separated. The real-time kinematic positioning (RTK) method was used to determine the UAV's coordinates. A reference 'base' station is used to correct the UAV's position. This method allows to obtain coordinates with a frequency of 20 Hz. The accuracy of UAV position determination is 10 mm in plan and 15 mm in height (Kazemeini et al. 2019).

The current state of development of an unmanned gamma monitoring system is presented in (Widodo et al. 2020). Gamma monitoring systems should be capable of mapping naturally high radiation backgrounds or areas contaminated with radionuclides, tracking the radioactive plume and searching for radioactivity sources. The radiation detection equipment should be an independent module. The module is proposed to use a semiconductor detector based on cadmium-zinc telluride (CdZnTe), which does not require a cooling system. The location monitoring module will consist of a GPS controlled by a microcontroller. A video camera can be installed on the UAV to visualize the location of the data. The modules should be powered by a battery the size of a smartphone. The collected data will be transmitted to a ground station located in the base camp in real time using the telemetry system of the radio frequency communication module.

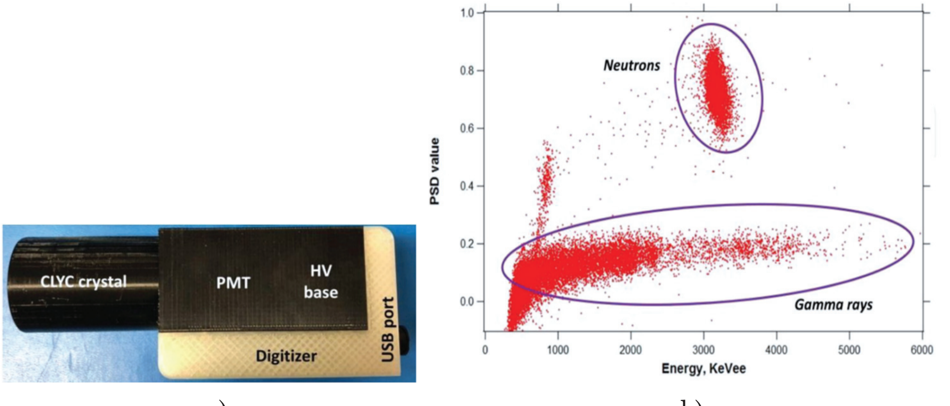

a) b)

Fig. 13. *Radiation detection sensors and neutron-gamma spectrogram: a) appearance of the CLYC sensor; b) neutron-gamma spectrogram (neutron-gamma plot) (Kazemeini et al. 2019).*

A method for determining the location of a radiation source G located on a flat earth surface A'B' is based on UAV control from a ground control station (Fig. 14) (Kryachok and Belenok 2023). UAV flight is performed on parallel, horizontally located trajectories, along which its coordinates, radiation dose rate, and UAV height above the earth's surface are measured synchronously and periodically. If the points A and B of maximum radiation power P_A, P_B with coordinates x_A, y_A , x_B, y_B , and heights above the earth's surface h_A, h_B are detected on two adjacent trajectories, the following calculations are performed at the ground station. Distance between opposite points of maximum radiation power

$$D = \sqrt{(x_B - x_A)^2 + (y_B - y_A)^2}\,, \tag{1}$$

ratio $a = \dfrac{P_A}{P_B}$, value $h = \dfrac{h_A + h_B}{2}$. Provided that $D \geq \dfrac{a-1}{\sqrt{a}}$, the horizontal distance from the maximum point A to the projection O on the horizontal surface of the radiation source G is calculated by the formula

$$d_{AO} = \frac{-D + \sqrt{D^2 - (a-1)\left[(a-1)h^2 - D^2\right]}}{a-1}\,, \tag{2}$$

$\alpha_{AB} = arctg\left(\dfrac{y_B - y_A}{x_B - x_A}\right)$ is the directional angle of the direction AB and the coordinates of the radiation source

$$x_0 = x_A + d_{AO}\cos\alpha_{AB}\,, \tag{3}$$

$$y_0 = y_A + d_{AO}\sin\alpha_{AB}\,. \tag{4}$$

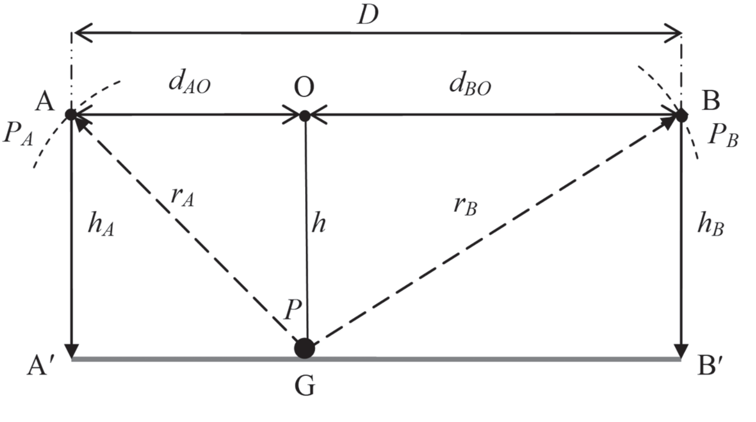

Fig. 14. *A method for determining the location of a radiation source (Kryachok and Belenok 2023).*

If $P_A = P_B$, then the coordinates of the radiation source are equal to the average of the corresponding coordinates x_A, y_A and x_B, y_B. Estimation of the radiation power at a distance of 1 m from the radiation source, taking into account the distance to the source $r_A = \sqrt{d_{OA}^2 + h^2}$, taken in meters, is equal to $P = P_A r_A^2$.

If $D < \frac{a-1}{\sqrt{a}}$, then, upon a command from the ground control station, the UAV flies along a horizontal trajectory between the opposite points of maximum radiation power *A* and *B*, and the planned coordinates and height *h'* of the detected point *C* of the maximum radiation power P_C on the flight path correspond to the location of the radiation source. The estimated power *P* of the radiation source at a distance of 1 m from it, taking into account the height *h'* taken in meters, is equal to $P = P_C(h')^2$ (Kryachok and Belenok 2023).

The application of this method requires a simplified mathematical apparatus for calculations. To determine the planned coordinates of the radiation source, it is not necessary to take into account air pressure and temperature to bring the altitude measurements to the earth's surface, since the method is based on the ratio of radiation powers measured on opposite routes at almost the same values of air parameters. The method can be implemented by a copter-type UAV with a payload in the form of a flight control system, a radio communication system with a ground station, an onboard GPS receiver, an altimeter, a mobile radiation detector with uniform sensitivity in the lower hemisphere, as well as an electronic system for controlling these devices and processing the results located at the ground control station.

4. Compton Imaging Systems on UAV Pplatforms

The remote radiation imaging system was developed for remote and rapid measurement of radioactive contamination inside the buildings of the Fukushima nuclear power plant (Sato et al. 2018). The system consisted of a multicopter with a Compton camera mounted on a gimbal; an on-board computer; an optical camera; a GPS receiver; and a battery (Fig. 15a).

The Compton camera consisted of three parts: a gamma ray detector, a signal processing unit, and an optical camera. The weight of the entire system did not exceed 1 kg. The gamma sensor consisted of two stages: a scatterer and an absorber (Fig. 15b). Each stage consists of a Ce-doped GAGG (Gd3Al2Ga3O12) scintillator combined with a multipixel photon counter. The distance between the scatterer and the absorber is 23.5 mm. The gamma sensor was connected to a signal processing unit that records and processes information about the position of the interaction of gamma quanta and the value of the energy released in the scatterer and absorber. The processed signals and optical images from the optical camera are transferred to a computer via a USB port.

a) b) c)

Fig. 15. *Remote radiation detection systems based on the Compton camera: a) the appearance of the remote radiation detection system; b) diagram of the gamma radiation detector; c) visualization of the 'hot spot' (Sato et al. 2018).*

Radiation images are reconstructed by the back-projection method and superimposed on optical images to visualize radioactive substances (Fig. 15c) (Sato et al. 2018).

The paper (Báča et al. 2021) presents the development of a new miniature system for the localization and assessment of compact gamma radiation sources on the platforms of mini rotary-wing aircraft (Fig. 16a).

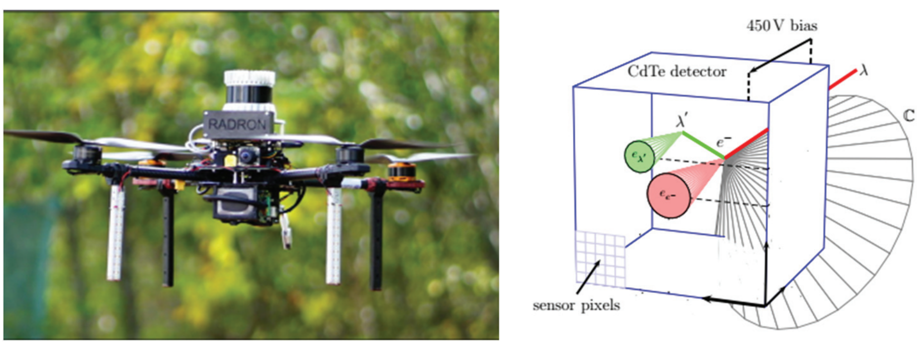

a) b)

Fig. 16. *Miniature localization system for detecting and evaluating compact gamma radiation sources: a) appearance of the system on a mini-UAV platform; b) illustration of the Compton scattering effect in a 2 mm thick CdTe detector with a voltage of 450 V, when the incoming gamma photon λ changes its momentum in the direction λ from the scattering center and forms an electron* e^- *(Báča et al. 2021).*

The system uses a single-sensor Compton chamber. The Compton chamber uses a cadmium telluride (CdTe) detector to measure Compton scattering products in the form of incoming high-energy gamma photons. The camera can also detect β particles and heavy ions. Particle traces can be classified to determine the nature of the radiation source. Unlike the dual-sensor camera (Sato et al. 2018), only one sensor is used to measure scattering products. For this purpose, a 2 mm thick semiconductor CdTe detector was used, capable of causing scattering effects in its thickness and also of capturing scattering products with a multi-pixel sensor (Fig. 16b) (Báča et al. 2021).

5. Conclusions

The article reviews the existing radiation imaging systems: with collimated detectors; with coded aperture; with rotational modulation; Compton imaging; with moving detectors. As a result, it becomes clear that Compton imaging systems and systems with moving detectors, due to their ability to operate in a remote radiation field and low weight characteristics, are currently suitable for use on UAV platforms.

The analysis of the peculiarities of using remote sensing tools for gamma monitoring in the form of systems with moving detectors and Compton imaging allows us to draw the following conclusions:

- systems with movable detectors allow for full gamma monitoring, namely, searching for radioactive sources, mapping of natural elevated radiation background and large areas contaminated with radionuclides;
- currently, Compton imaging systems allow detecting sources of radiation sources at lower altitudes and speeds with a delay above the over the source for its identification, which makes them effective for searching for sources in local areas of the urban environment and indoors, but not allows mapping of large areas of radiation contamination.

ACKNOWLEDGEMENTS. The author Lillia Hebryn-Baidy express gratitude to the British Academy and the Council for At-Risk Academics for support to this research through the Researchers at Risk Research Support Grants.

References

Adão, T., Hruška, J., Pádua, L., Bessa, J., Peres, E., Morais, R., Sousa, J. J. (2017): Hyperspectral imaging: A review on UAV-based sensors, data processing and applications for agriculture and forestry, Remote Sensing, 9 (11), 1110, https://doi.org/10.3390/rs9111110.

Ahmad, M. I., Ab. Rahim, M. H., Nordin, R., Mohamed, F., Abu-Samah, A., Abdullah, N. F. (2021): Ionizing Radiation Monitoring Technology at the Verge of Internet of Things, Sensors, 21 (22), 7629, https://doi.org/10.3390/s21227629.

Amgarou, K., Paradiso, V., Patoz, A., Bonnet, F., Handley, J., Couturier, P., Becker, F., Menaa, N. (2016): A comprehensive experimental characterization of the iPIX gamma imager, Journal of Instrumentation, 11 (8), P08012, https://doi.org/10.1088/1748-0221/11/08/P08012.

Báča, T., Štibinger, P., Doubravova, D., Turecek, D., Solc, J., Rusnak, J., Saska, M., Jakubek, J. (2021): Gamma Radiation Source Localization for Micro Aerial Vehicles with a Miniature Single-Detector Compton Event Camera, 2021 International Conference on Unmanned Aircraft Systems, ICUAS 2021, 338–346, 9476766, https://doi.org/10.1109/ICUAS51884.2021.9476766.

Burachek, V., Malik, T., Kryachok, S., Bryk, Y., Belenok, V. (2018): Device for automated leveling, News of the Academy of Sciences of the Republic of Kazakhstan. Series of geology and technical sciences, 5 (431), 95–99, https://doi.org/10.32014/2018.2518-170X.13.

Burtniak, V., Zabulonov, Y., Stokolos, M., Bulavin, L., Krasnoholovets, V. (2018): Application of a territorial remote radiation monitoring system at the Chornobyl nuclear accident site, Journal of Applied Remote Sensing, 12 (4), 046007, https://doi.org/10.1117/1.JRS.12.046007.

Chen, C. M., Sinclair, L. E., Fortin, R., Coyle, M., Samson, C. (2020): In-Flight Performance of the Advanced Radiation Detector for UAV Operations (ARDUO), Nuclear Instruments and Methods in Physics Research, Section A: Accelerators, Spectrometers, Detectors and Associated Equipment, 954, 161609, https://doi.org/10.1016/j.nima.2018.11.068.

Galushko, A. (2023): A fleet of drones and the new naval warfare, https://www.blackseanews.net/en/read/200783, (accessed 5 August 2024).

Gordon, G. (2008): Practical Gamma-ray Spectrometry, 2nd Edition, Wiley, Warrington, UK, https://nna1989.files.wordpress.com/2015/05/gordon-gilmore-practical-gamma-ray-spectroscopy-2008.pdf, (accessed 5 August 2024).

Kazemeini, M., Vargas, J., Barzilov, A., Yim, W. (2019): Gamma Ray Measurements Using Unmanned Aerial Systems, Use of Gamma Radiation Techniques in Peaceful Applications, http://dx.doi.org/10.5772/intechopen.82798.

Korsunov, S., Volkov, A., Oboronov, M., Oriekhov, S., Gurtovenko, V., Fedchenko, S. (2021): Transformation of unmanned aviation tasks from its creation to application in modern military conflicts, Development, combat application and armament of aviation, 3 (44), 66–81, https://doi.org/10.30748/nitps.2021.44.08, (in Ukrainian).

Kryachok, S. (2024): Application of unmanned aerial vehicles for radiation monitoring, Technical Sciences and Technologies, 3 (37), https://doi.org/10.25140/2411-5363-2024-3(37)-247-261, (in Ukrainian).

Kryachok, S. D., Belenok, V. Iu. (2023): Method for determining the location of a radiation source, Utility model patent No. 154278, Ukraine, PMK (2023.1) C 7/00, G01C 3/00. Applied for 3.2.2023; Published 1.11.2023; Bulletin No. 44, 6 p. (in Ukrainian).

Kunze, C., Preugschat, B., Arndt, R., Kandzia, F., Wiens, B., Altfelder, S. (2022): Development of a UAV-Based Gamma Spectrometry System for Natural Radionuclides and Field Tests at Central Asian Uranium Legacy Sites, Remote Sensing, 14 (9), 2147, https://doi.org/10.3390/rs14092147.

Makhnov, O. I. (2019a): Development of the optimal design of a gamma radiation imaging system, Electronic and Acoustic Engineering: scientific and technical journal, 2 (3), 6–10, https://doi.org/10.20535/2617-0965.2019.2.3.163436, (in Ukrainian).

Makhnov, O. I. (2019b): Gamma radiation visualization system. Diploma project, https://ela.kpi.ua/bitstream/123456789/28084/1/Makhnov_bakalavr.pdf, (accessed 5 August 2024) (in Ukrainian).

Molnar, A., Domozi, Z., Lovas, I. (2021): Drone-based gamma radiation dose distribution survey with a discrete measurement point procedure, Sensors, 21 (14), 4930, https://doi.org/10.3390/s21144930.

Paradiso, V., Amgarou, K., Lanaute, N. B. D., Schoepff, V., Amoyal, G., Mahe, C., Beltramello, O., Liénard, E. (2017): A panoramic coded aperture gamma camera for radioactive hotspots localization, Journal of Instrumentation, 12 (11), P11010, https://doi.org/10.1088/1748-0221/12/11/P11010.

Pavlovsky, R., Haefner, A., Joshi, T. H., Negut, V., McManus, K., Suzuki, E., Barnowski, R., Vetter, K. (2018): 3-D Radiation Mapping in Real-Time with the Localization and Mapping Platform LAMP from Unmanned Aerial Systems and Man-Portable Configurations, https://www.semanticscholar.org/reader/751a68f57b684c6cf3a1e6de3f6c42a5a321e144, (accessed 5 August 2024).

Sato, Y., Ozawa, S., Terasaka, Y., Kaburagi, M., Tanifuji, Y., Kawabata, K., Miyamura, H. N., Izumi, R., Suzuki, T., Torii, T. (2018): Remote radiation imaging system using a compact gamma-ray imager mounted on a multicopter drone, Journal of Nuclear Science and Technology, 55 (1), 90–96, https://doi.org/10.1080/00223131.2017.1383211.

Silwal, A., Tamang, S., Adhikari, R. (2022): Use of unmanned aerial vehicle (UAV) formapping, and accuracy assessment of the orthophoto with and without using GCPs: A case study in Nepal, Mersin Photogrammetry Journal, 4 (2), 45–52, https://doi.org/10.53093/mephoj.1176847.

Tereshchuk, O. I., Kryachok, S. D., Belenok, V. Iu., Malik, T. M., Hebryn-Baidy, L. V. (2021): Robotic complex for the runway leveling. Device for automated leveling. News of the Academy of Sciences of the Republic of Kazakhstan. Series of geology and technical sciences, 2 (446), 180–188, https://doi.org/10.32014/2021.2518-170X.51.

Tereshchuk, O., Kryachok, S., Belenok, V., Boyko, O., Alpert, S. (2023): Improvement of the method of verification of the drift of the gyrovertical on the UAV during aerial photography using the liquid horizon, Remote Sensing Applications: Society and Environment, 32, 101045, https://doi.org/10.1016/j.rsase.2023.101045.

Van der Veeke, S., Limburg, J., Koomans, R. L., Söderström, M., de Waal, S. N., van der Graaf, E. R. (2021): Footprint and height corrections for UAV-borne gamma-ray spectrometry studies, Journal of Environmental Radioactivity, 231, 106545, https://doi.org/10.1016/j.jenvrad.2021.106545.

Vetter, K., Mihailescu, L., Nelson, K., Valentine, J., Wright, D. (2006): Gamma-ray Imaging Methods, Technical Report, https://doi.org/10.2172/1036848.

Widodo, S., Abimanyu, A., Apribra, R. (2020): Development of drone mounted aerial gamma monitoring system for environmental radionuclide surveillance in BATAN, J. Phys., Conf. Ser. 1436 012126, https://doi.org/10.1088/1742-6596/1436/1/012126.

Woodbridge, E., Connor, D. T., Verbelen, Y., Hine, D., Richardson, T., Scott, T. B. (2023): Airborne gamma-ray mapping using fixed-wing vertical take-off and landing (VTOL) uncrewed aerial vehicles, Frontiers in Robotics and AI, 10, 1137763, https://doi.org/10.3389/frobt.2023.1137763.

Zabulonov, Yu. L., Burtnyak, V. M., Odukalets, L. A. (2017): System for Effective Remote Control and Monitoring of Radiation Situation Based on Unmanned Aerial Vehicle, Science and Innovation, 13 (4), 46–53, http://dx.doi.org/10.15407/scin13.03.046, (in Ukrainian).

Zhang, L., Zhang, H., Niu, Y., Han, W. (2019): Mapping maize water stress based on UAV multispectral remote sensing, Remote Sensing, 11 (6), 605, https://doi.org/10.3390/rs11060605.

Zhyrokhov, M. (2017): Ground drones: the main achievements of the Ukrainian defense industry, https://mind.ua/openmind/20177877-nazemni-droni-golovni-dosyagnennya-ukrayinskogo-oboronpromu, (accessed 22 April 2025) (in Ukrainian).

URLs

URL 1: REMUS underwater drones will help ships break through sea minefields, https://sundries.news/remus-underwater-drones-will-help-ships-break-through-sea-minefields/, (accessed 5 August 2024).

URL 2: Ground Drone XAG R150 2022 XAUV RevoMower, https://store.drone.ua/nazemnyi-dron-xag-r150-2022-xauv-revomower/, (accessed 5 August 2024) (in Ukrainian).

Osobitosti primjene sustava vizualizacije na platformama UAV-a za daljinsko praćenje gama zračenja

SAŽETAK. Trenutačno je povećana prijetnja od upotrebe nuklearnog oružja, njegovim raspoređivanjem u novim regijama, a postoje i rizici od nesreća u nuklearnim elektranama i terorističkih akcija koji uključuju nuklearna punjenja. Stoga je relevantno daljinsko praćenje gama zračenja. Sposobnost bespilotnih letjelica da lete na niskim visinama i brzinama omogućuje povećanje pouzdanosti praćenja gama zračenja u usporedbi s letjelicama s posadom za daljinska istraživanja te da zaštite operatere bespilotnih letjelica od izloženosti zračenju u usporedbi s metodama na tlu, dok vizualizacija rezultata praćenja osigurava dvodimenzionalne ili trodimenzionalne modele raspodjele zračenja na Zemljinoj površini. Pregled sustava snimaka zračenja provodi se: pomoću kolimiranih detektora, kodiranog otvora, rotacijske modulacije, Comptonova sustava snimanja, pokretnih detektora (usmjerenih sustava). Zbog najmanjih veličina i mase te sposobnosti rada u udaljenom gama polju, samo su posljednja dva sustava trenutačno prikladna za uporabu na bespilotnim letjelicama. Utvrđeno je da sustavi s pokretnim detektorima na platformama UAV-a omogućuju praćenje gama zračenja u cijelosti: traženje izvora radioaktivnosti, kartiranje pozadine prirodnog zračenja i područja kontaminiranih radionuklidima. Trenutačno, Comptonovi sustavi snimanja omogućuju otkrivanje izvora zračenja na nižim visinama i brzinama, što ih čini učinkovitima za traženje izvora u lokalnim područjima urbanog okoliša te u zatvorenom prostoru, ali ne dopuštaju kartiranje velikih područja kontaminacije zračenjem.

Ključne riječi: sustavi snimanja, gama zračenje, daljinska istraživanja, bespilotne letjelice, detektori gama zračenja, praćenje zračenja.

Received / Primljeno: 2025-01-19

Accepted / Prihvaćeno: 2025-04-22